

Time Evolution of the Shear Layer of a Supersonic Axisymmetric Jet

D. C. Fourquette*

Wellesley College, Wellesley, Massachusetts 02181

M. G. Mungal†

Stanford University, Stanford, California 94305

and

R. W. Dibble‡

Sandia National Laboratories, Livermore, California 94550

We used a two-laser two-detector experiment to investigate the temporal evolution of the mixing layer of a pressure matched supersonic jet at an exit Mach number of 1.5, discharging into still air, resulting in a convective Mach number of 0.7. The convective speed of the structures present in the flow was measured and compared with previous findings. Additional views of the mixing layer provided information on the three dimensionality of the mixing layer. We found that the structures travel with a velocity higher than the predicted velocity and they rotate as they progress downstream.

Introduction

WITH the renewed interest in compressible flows, several important flowfields are presently under experimental investigation. These include two-dimensional mixing layers,¹⁻⁶ coflowing jets,^{7,8} and jets in crossflow.⁹ For the two-dimensional mixing layer it has been shown¹⁻⁵ that, as the difference in velocity between the two streams increases and compressibility becomes important, the shear layer growth rate is drastically reduced, and consequently so is the amount of mixed gases at the fluid interface. Such results have been obtained to date primarily by means of flow visualization using the schlieren technique,¹⁻⁴ intrusive pitot tubes, and laser Doppler velocity (LDV) measurements.⁴

There have also been earlier laser-based attempts to measure the velocity via LDV¹⁰ and temperature and density¹¹ via Raman scattering. However, these attempts produced only time averaged quantities. More recent experiments have used Rayleigh scattering¹¹ and laser-induced fluorescence^{9,13,14} to extract instantaneous measures.

In this study we applied the two-dimensional laser Rayleigh scattering technique, already used successfully in other flows,¹⁵ to instantaneously visualize a pressure-matched supersonic air jet discharging into still air. The goals of this work were to investigate the evolution of the shear layer and to provide better understanding of supersonic mixing. In particular, time lapse images were taken to study the convective speed of the large-scale structures in order to compare it with the recent findings of Papamoschou.² Additional findings concerning the two dimensionality of the structure of the mixing layer of a round jet are also provided.

Experimental Conditions

Figure 1 shows a schematic of the experimental setup. To eliminate shocks, a convergent-divergent nozzle was designed

to produce a flow exit Mach number of 1.5 at atmospheric pressure. The jet fluid consisted of air at 300 K stagnation temperature and a relative humidity of 8%, which entrained surrounding still air at 300 K and 40% relative humidity. The calculated exit velocity was 430 m/s at a static temperature of 210 K. The diameter of the sonic section was 8 mm; therefore, the Reynolds number based on throat conditions was 4.6×10^5 . While the jet exit Mach number was 1.5, the convective Mach number M_c (Refs. 1 and 16) was 0.7, suggesting that the flow was well into the compressible range. Tam and Hu¹⁷ have shown that three families of instability waves are possible in high-speed jets, but for our conditions here (low supersonic Mach number) only the Kelvin-Helmholtz instability is expected to be active.

Two frequency doubled Nd:Yag laser beams were formed into coplanar sheets, which illuminated the same region of the flow containing the jet axis. The light scattered off of each illuminated plane was collected through a lens and then imaged onto the face of one of two computer-controlled Charge Coupled Device (CCD) detectors used for the experiment. The

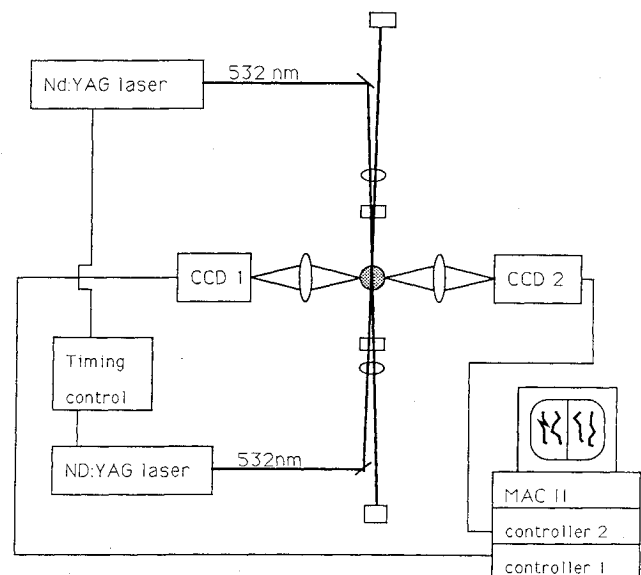


Fig. 1 Experimental setup.

Received Nov. 8, 1989; presented as Paper 90-0508 at the AIAA 28th Aerospace Sciences Meeting, Reno, NV, Jan. 8-11, 1990; revision received June 20, 1990; accepted for publication June 20, 1990. Copyright © 1990 by the American Institute of Aeronautics and Astronautics, Inc. All rights reserved.

*Assistant Professor, Department of Physics. Member AIAA.

†Assistant Professor, Mechanical Engineering Department. Member AIAA.

‡Senior Member, Technical Staff; currently Associate Professor, at Mechanical Engineering Department, University of California, Berkeley, CA 94720.

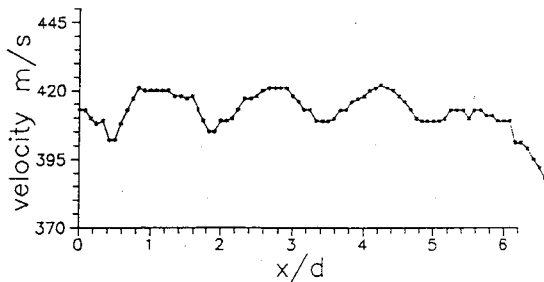


Fig. 2 Streamwise velocity along the centerline.

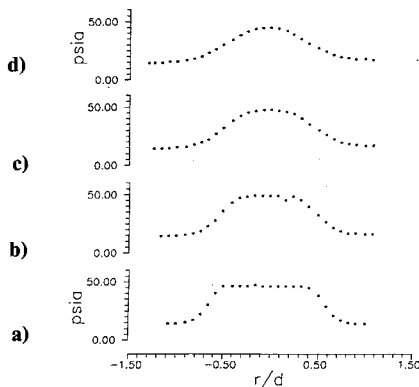


Fig. 3 Radial pitot pressure profiles: a) at $x/D = 3$; b) at $x/D = 4$; c) at $x/D = 5$; d) at $x/D = 6$.

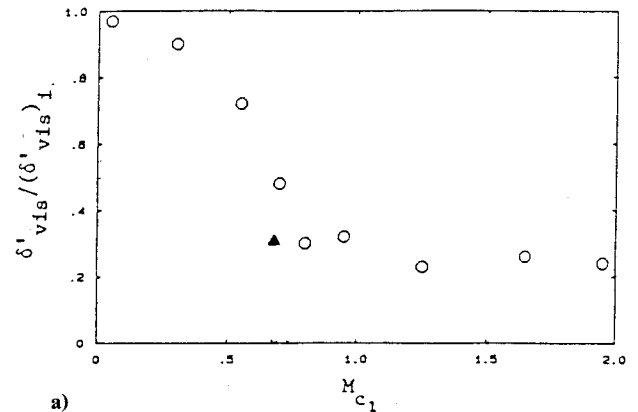
lasers were triggered with a variable time interval, typically consisting of a few microseconds. Each CCD detector was gated to see the scattered light of only one beam, thus producing two sequential images of the solution of the shear layer. The time duration of each laser pulse was 10 ns, sufficient to freeze the motion. Each image was recorded as a digitized array of 576×384 values (maximum size of the CCD active area). The physical size of the imaged region was $30 \times 20 \times 0.30$ mm. The advantages of the digital data are that it is now possible to easily highlight flow features (e.g., via false color) and perform subsequent calculations of the convective speed of organized structures.

A novel aspect of this work, and the work reported in Ref. 12, is that, when the cold jet fluid mixed with the surrounding air, condensation occurred and formed fine water droplets.¹⁸ The maximum size for the droplet to accurately follow the flow was recently investigated by Samimy and Lele.¹⁹ Calculations indicated that the maximum particle size in our case was 300 nm. If we assume that all of the water vapor contained in the probe volume condenses into $n = 10^3$ water molecules, similar to the calculations described in Ref. 20, then the maximum size of each droplet cannot exceed 350 nm in diameter. This number n is a conservative estimate since below that number the marker shot noise of the data would be quite noticeable. Therefore, we believe that the motion of the water particles represents the flowfield accurately.

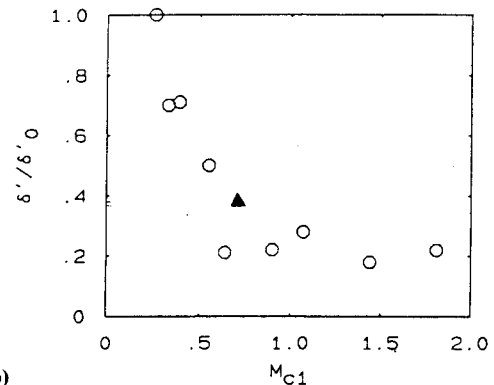
Results and Discussion

Pitot Tube Measurements

Stagnation pressure measurements along the jet axis were performed in order to verify the uniformity of the velocity. Figure 2 shows the velocity profile between 0 and 6.2 nozzle diameters downstream. The velocity fluctuation was found to be about 2%. These variations are attributed to weak shocks, which are a consequence of our nozzle contour. Transverse stagnation pressure measurements between 3 and 6 diameters are shown in Fig. 3. These profiles exhibit good symmetry with respect to the jet axis.



a)



b)

Fig. 4 Normalized visible shear layer growth rate as function of convective Mach number: a) visible growth rate (circles from Papamoschou and Roshko¹; triangle from this work); b) pitot tube measurements (circles from Papamoschou²; triangle from this work).

Growth Rate Measurements

Figures 4a and 4b show the ratio of the visible compressible shear layer growth rate to that of the incompressible layer at the same density and speed ratios as a function of the convective Mach number.¹ The compressible shear layer growth was measured by ensembles averaging 20 individual events (see sec. on three dimensionality) and graphically obtaining the growth angle in the region before the end of the potential core. An additional value of the growth rate was also obtained using the pitot tube data shown in Fig. 3. For each location downstream the 5 and 95% width was found and the growth rate calculated. The result is compared with the findings of Papamoschou² and shown in Fig. 4b. As a verification, the growth rate was obtained from ensemble-averaged transverse views (see the subsection on three dimensionality) and generally agrees with our growth angle finding. Our data points in Fig. 4 suggest that the present layer is one that is undergoing significant compressibility effects and is most likely representative of two-dimensional turbulent mixing layers. It is important to note that our measurement technique utilizes the scalar mixing field and is somewhat different from the schlieren measurements used to generate the data in Ref. 1.

Time Lapse Imaging Results

Two-laser, two-detector experiments were performed for a range of time delays varying from 2 to 20 μ s as described in the preceding section. Figures 5–8 show the two sequential images from both cameras for different time delays. The flow direction is from bottom to top, with each frame extending from 2.8 to 6.0 nozzle diameters downstream. Each frame shows the mixing layer that borders the central potential core with the centerline of the jet appearing toward the right of each image.

Figures 5a and 5b show two resulting images at a time interval of 7.8 μ s. The hexagonal pattern visible in each image is due to the fiber-optic coupler between the image intensifier

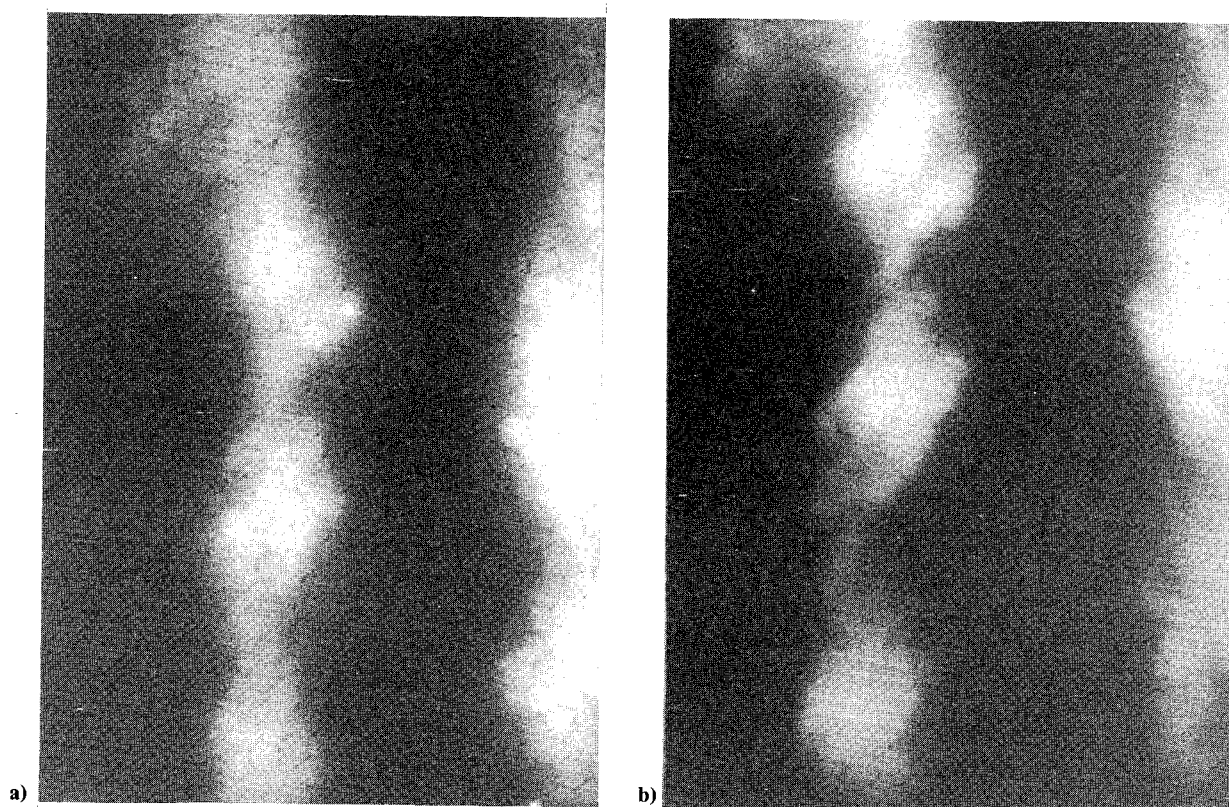


Fig. 5 Time lapse photographs of mixing layer. Time interval = $7.8 \mu\text{s}$.

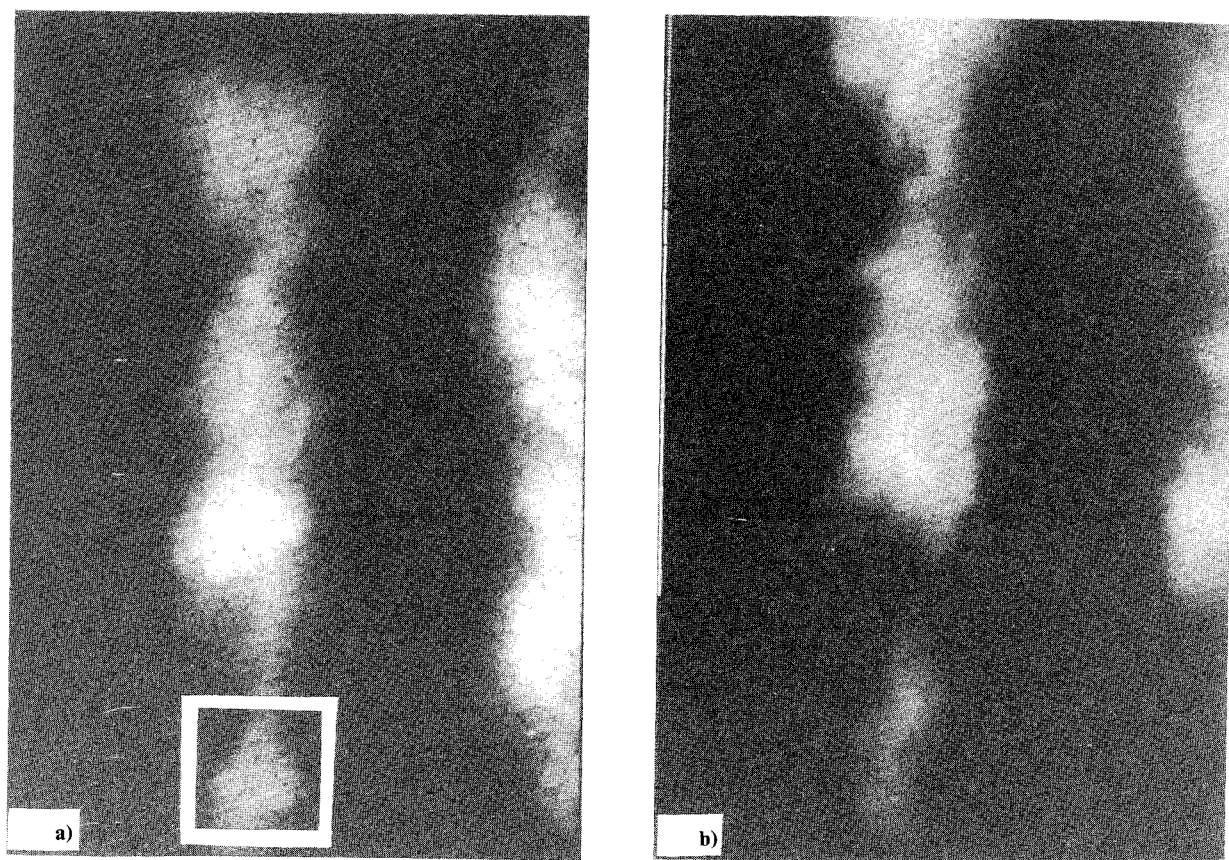


Fig. 6 Time lapse photographs of mixing layer. Time interval = $11.7 \mu\text{s}$.

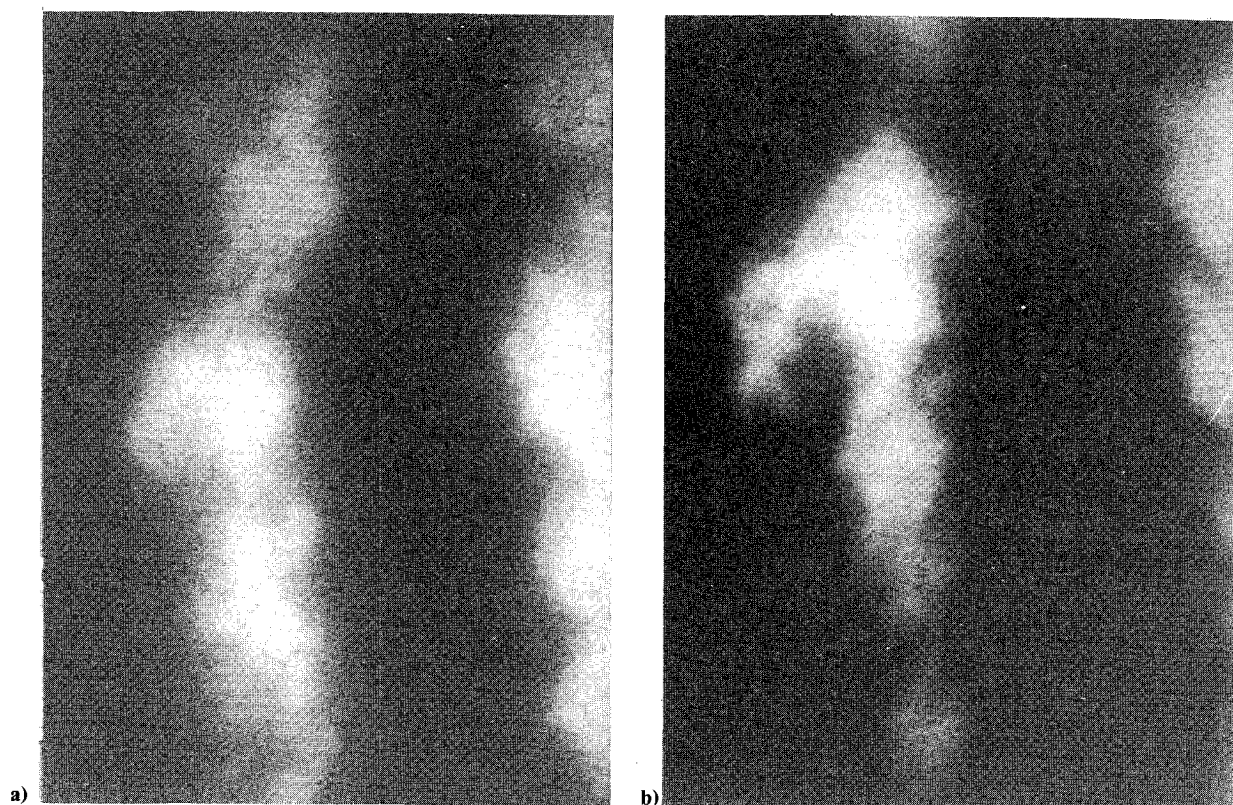


Fig. 7 Time lapse photographs of mixing layer. Time interval = $15.7 \mu\text{s}$.

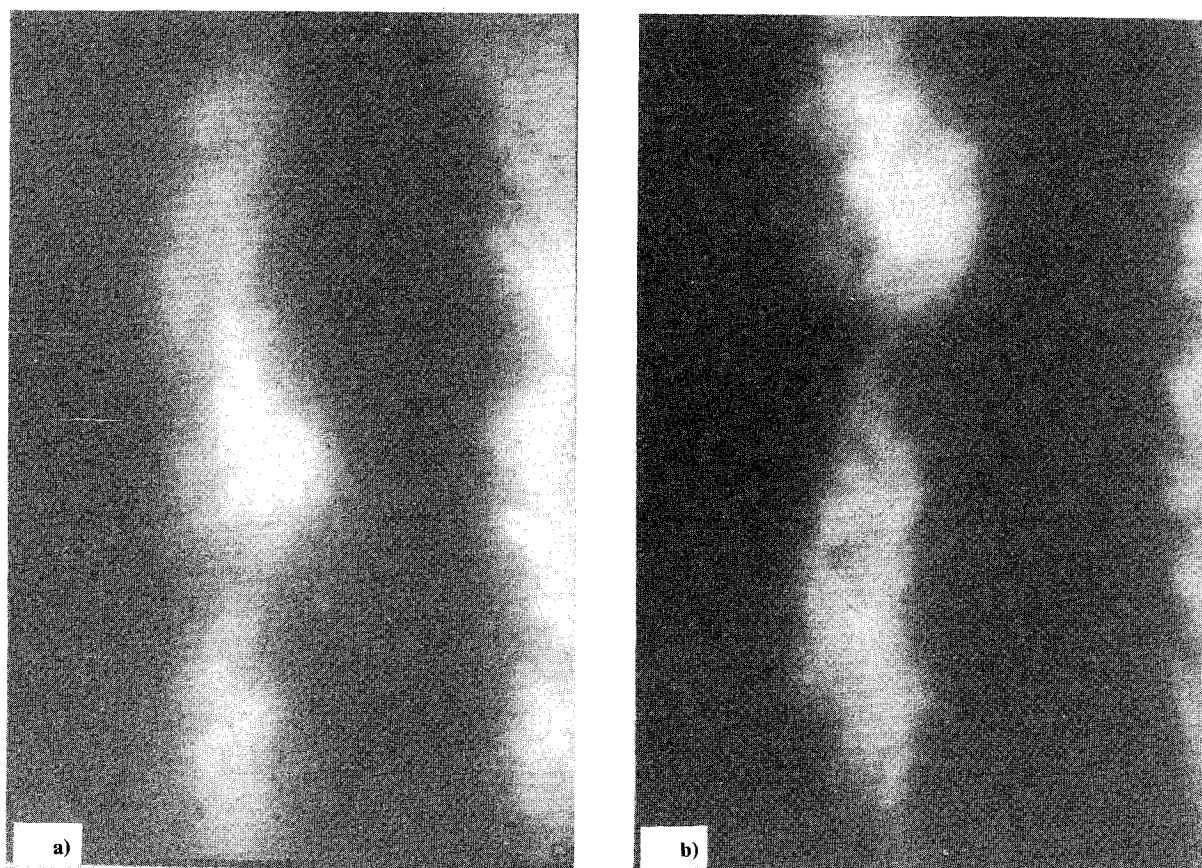


Fig. 8 Time lapse photographs of mixing layer. Time interval = $20 \mu\text{s}$.

and the CCD array and can be ignored for our purposes. Two features are readily apparent: 1) the existence of large-scale mixing regions or structures that span the width the mixing layer and 2) the translation of the structure as it progresses downstream. Such features were first noted by Papamoschou² in his double-pulse schlieren images, but whereas his approach tended to emphasize distinct features at the edge of the shear layer, our technique emphasizes the cross section of a given structure. Figures 6–8 show similar results for increasing time delay. It is now much more apparent that considerable solution of the structure occurs (viz., deformation and rotation) in conjunction with the obvious translation. For example, in Fig. 8, at a time delay of 20 μ s, the structure has traveled approximately one local structure length and rotated about 20 deg. Such features were not readily noted using the schlieren technique in Ref. 2 and probably has to do with the fact that the line-of-sight approach is not well suited to revealing detailed features of the flow.

Connective Velocity Measurements

Papamoschou and Roshko¹ and Bogdanoff¹⁶ introduced the idea of the convective speed of the large-scale structure, U_c . For the case of equal specific heat ratios of the low-speed and high-speed fluids, the theoretical formula for the convective speed is¹

$$U_c = \frac{a_2 * U_1 + a_1 * U_2}{a_1 + a_2} \quad (1)$$

leading to the convective Mach numbers

$$M_{c1} = \frac{U_1 - U_c}{a_1} \quad (2)$$

and

$$M_{c2} = \frac{U_c - U_2}{a_2} \quad (3)$$

where a_1 and a_2 are the speed of sound in the two fluids, and U is the flow velocity. In a series of experiments designed to measure the actual experimentally observed U_c , Papamoschou² showed that, for values of the convective Mach number less than 0.4 (i.e., incompressible behavior), there is good agreement between the theoretical prediction and the experimentally observed value, whereas for convective Mach numbers above 0.4 (i.e., compressible behavior), a discrepancy exists between the theoretical and experimental values.

Images such as Figs. 5–8 provide the data necessary to compute the convective speed of particular events, and this provides independent measures of the actual convective speed. In order to calculate the convective velocity of the structures with a minimum of bias, we developed a computational method that takes into account the large-scale structure as a whole. The digital nature of the data made such computations possible. For a pair of events, subsequently referred to as E_0 and E_1 , a subarray S_0 containing a characteristic pattern in the shear layer was isolated in E_0 and the autocorrelation A between the subarray and the shear layer in E_0 was calculated along the flow direction using the following formula:

$$A(k,j) = \frac{\text{SUM}_i [S_0(i,j) \times E_0(i+k,j)]}{\text{SUM}_i [S_0(i,j) \times S_0(i,j)]} \quad (4)$$

The cross correlation C was then calculated between the subarray S_0 and E_1 using the following method:

$$C(k,j) = \frac{\text{SUM}_i [S_0(i,j) \times E_1(i+k,j)]}{\text{SUM}_i [S_0(i,j) \times S_0(i,j)]} \quad (5)$$

Figure 9 shows the results of the autocorrelation and cross correlation for a pair of events 11.7 μ s apart shown in Figs. 6a and 6b. The subarray used for this calculation is represented

by the subwindow in Fig. 6a. The connective speeds, calculated to be 294 m/s for the first structure \blacktriangle and 285 m/s for the second one \otimes , are higher than the theoretical value, 230 m/s. Also, the resemblance between the autocorrelation and crosscorrelation curves indicates that the structures have moved with similar velocities.

Figure 10 shows the autocorrelation and crosscorrelation for the pair of events presented in Figs. 8a and 8b. The convective velocity of the first structure was found to be 244 and 494 m/s for the second structure. The much larger than expected convective velocity for the second structure (exceeding the centerline velocity) illustrates the limitations of the computational method, i.e., it does not take rotational motion into account. Nevertheless, averaging over 36 measurements our calculated convective speed is 352 m/s, higher than the theoretical value of 230 m/s. From these measurements we conclude that the high-speed convective Mach number, $M_{c1} = 1.0$, and the low-speed convective Mach number, $M_{c2} = 0.24$ are different from the theoretical values, $M_{c1} = M_{c2} = 0.7$. These results are consistent with Papamoschou's² recent results, in the sense that the convective speed is not equal to the theoretical value, and agrees with his established trend for supersonic/subsonic shear layers. Interestingly, these results are less in accord with the prediction of Sandham²¹ (302 m/s for our experimental conditions), who computed the convective speed of the neutrally amplified wave and found the same trend as Papamoschou, but with less dramatic deviation from the theoretical value. We conclude from these measurements that for our conditions the convective speed is clearly larger than the theoretical value and generally supportive of Papamoschou's results.

Three Dimensionality

Papamoschou² conjectured that a possible explanation of the difference between theoretical and experimental convective speeds might be the presence of shocklets in the flow,

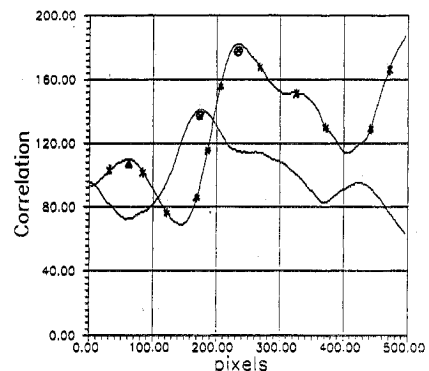


Fig. 9 Autocorrelation and crosscorrelation (asterisks) for a pair of events from Fig. 6.

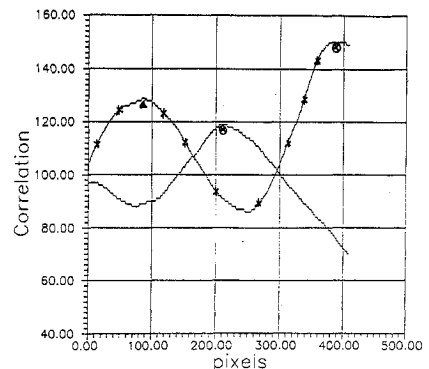


Fig. 10 Autocorrelation and crosscorrelation (asterisks) for a pair of events from Fig. 8.

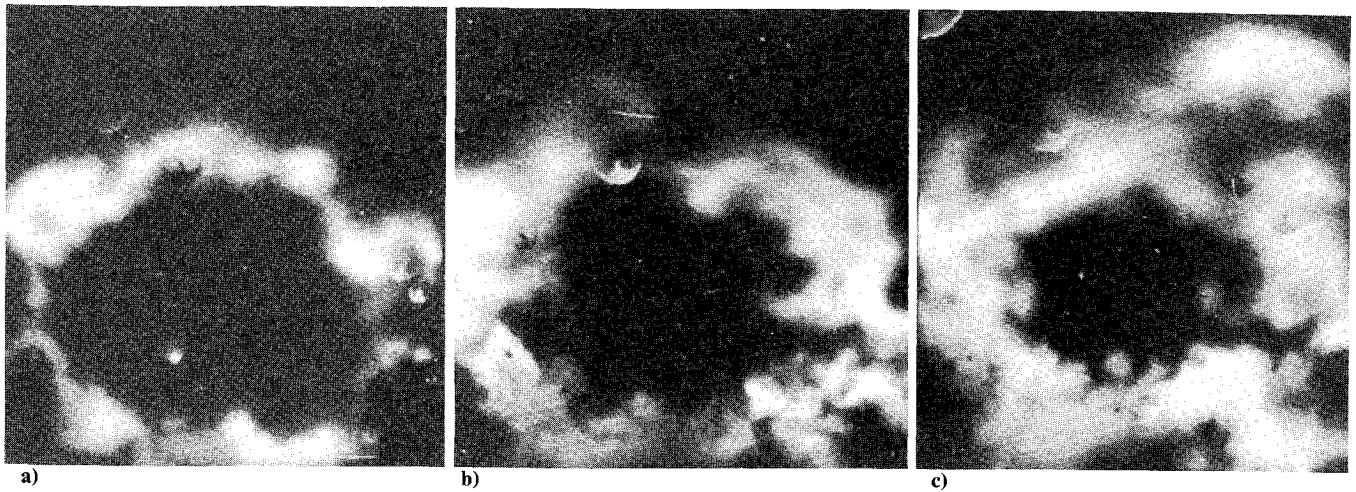


Fig. 11 Instantaneous azimuthal views of the jet: a) $x/D = 3.1$; b) $x/D = 4.7$; c) $x/D = 6.2$.

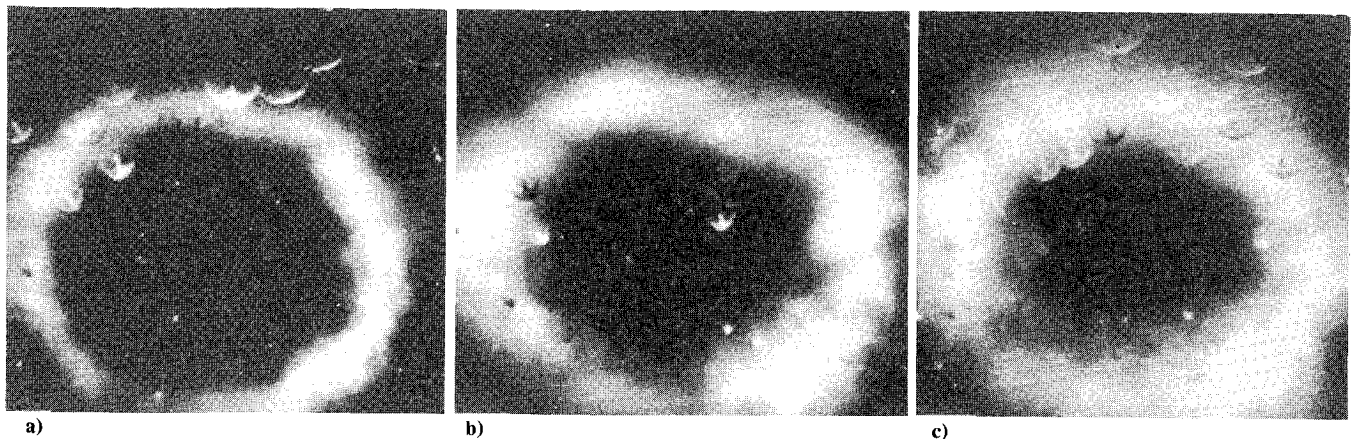


Fig. 12 Ensemble-averaged azimuthal views of the jet: a) $x/D = 3.1$; b) $x/D = 4.7$; c) $x/D = 6.2$.

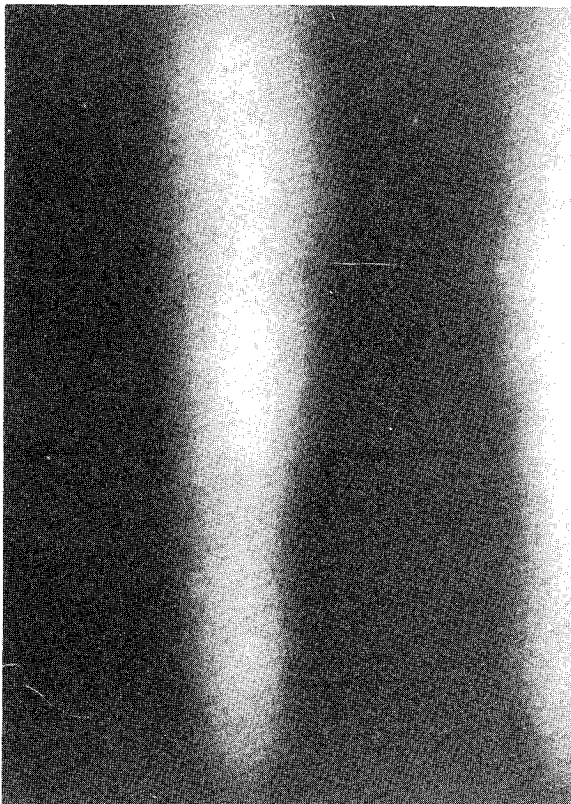


Fig. 13 Ensemble-averaged streamwise views of the jet.

whereas Sandham,²¹ Sandham and Reynolds,²² and Ragab and Wu²³ suggest that oblique mode instabilities are more likely at play under compressible conditions leading to potentially greater three dimensionality. In order to address the question of such three dimensionality of the compressible mixing layer, additional views of the flow were taken using the present technique. Figures 11a-c show time-independent azimuthal views of the flow under the same experimental conditions as those described earlier. To record these images, the planar laser sheet was made to intersect the jet in a plane perpendicular to the flow direction. The scattered light was collected by a lens whose optical axis made a 30-deg angle with the jet axis. Thus, there is some optical distortion and lack of focusing away from the focal axis which in these images corresponds to the 10 o'clock to 4 o'clock line. Examination of these images shows that the organized structure is by no means two dimensional (ring like) in extent but consists of local regions of activity. Regions where little or no condensation exists can be observed in the shear layer as well as optical structures. It is clear from these views that the structures presented in Figs. 5-8 are not axisymmetric around the jet axis, and that they do not necessarily convert primarily in the downstream direction.

Ensemble-averaged images such as Fig. 12 were also obtained and show the usual structureless, linearly spreading flow discussed in Fig. 4. Such images also show that the spreading rate determined by either images such as Fig. 12 or Fig. 13 lead to essentially the same result.

To confirm the findings in Fig. 11, a tangential view of the jet was obtained by moving the probe volume off the jet axis and illuminating the shear layer itself (Fig. 14). Well-defined streamwise structures can clearly be observed. Similar three-



Fig. 14 Three examples of tangential views of the shear layer.

dimensional features of the flow structure are also apparent in the study of Clemens et al.²⁴ in a compressible two-dimensional mixing layer, further confirming the idea that the present results are representative of two-dimensional mixing layers in general. Oblique waves reduce the convective Mach number by the cosine of the wave angle, therefore reducing the compressibility effects.² We note that obliquity of the waves also is observed in recent numerical simulations by Sandham and Reynolds,²² who also showed that shocklets do not appear when oblique waves are present. More importantly, three-dimensional calculations do not show the presence of shocks, at least for $M_c < 1.05$, the highest value computed.

Conclusions

These experiments have examined the shear layer development of a round matched supersonic jet using laser-based Rayleigh scattering techniques. This appearance of finely condensed moisture greatly increased the signal, allowing easier observation of flow structures. The observed features are believed to be representative of two-dimensional mixing layers in the sense that our visual growth rate agrees well with the visual measurements of Papamoschou² and Roshko.¹ Convective speeds of organized structures are measured using two-laser, two-camera techniques and suggest values that are different from the theoretical value, in general agreement with the findings of Papamoschou. We also note considerable evolution of the structure as it progresses downstream as revealed by the overall distortion of the same structure. Finally, views of the layer reveal a flowfield that is considerably more three dimensional than its incompressible counterpart. The three-dimensional aspect is generally consistent with the recent findings of Clemens et al.²⁴ in a two-dimensional mixing layer at a convective Mach number of 0.6. Our findings are in general agreement with those of Papamoschou and Roshko¹ and Papamoschou,² except that in our planar technique we observe rotation of structures that may be obscured in the line-of-sight schlieren technique.

Acknowledgments

This work was supported by the U.S. Department of Energy, Office of Basic Energy Sciences, Division Chemical Sciences. D. C. Fourquette was partially supported by Associated Western Universities.

References

- ¹Papamoschou, D., and Roshko, A., "Observations of Supersonic Free Shear Layers," AIAA Paper 86-0162, Jan. 1986; also "The Compressible Turbulent Shear Layer: an Experimental Study," *Journal of Fluid Mechanics*, Vol. 197, 1988, pp. 453-477.
- ²Papamoschou, D., "Structure of the Compressible Turbulent Shear Layer," AIAA Paper 89-0126, Jan. 1989.
- ³Brown, G., and Roshko, A., "On Density Effects and Large Scale Structure in Turbulent Mixing Layers," *Journal of Fluid Mechanics*, Vol. 64, 1974, pp. 774-816.
- ⁴Chinzei, N., Masuya, G., Komuro, T., Murakami, A., and Kudou, K., "Spreading of Two-Stream Supersonic Turbulent Mixing Layers," *Physics of Fluids*, Vol. 29, No. 5, 1986, pp. 1345-1347.
- ⁵Samimy, M., and Elliot, G. S., "Effects of Compressibility on the Structure of Free Shear Layers," AIAA Paper 88-3054A, July, 1988.
- ⁶Shau, Y. R., and Dolling, D. S., "Experimental Study of Spreading Rate Enhancement of High Mach Number Turbulent Shear Layers," AIAA Paper 89-2458, July, 1989.
- ⁷Gutmark, E., Schadow, K. C., and Wilson K. J., "Mixing Enhancement in Coaxial Supersonic Jets," AIAA Paper 89-1812, July, 1989.
- ⁸Naughton, J., Cattafesta, L., and Settles, G., "An Experimental Study of the Effect of Streamwise Vorticity on Supersonic Mixing Enhancement," AIAA Paper 89-2456, July, 1989.
- ⁹McDaniel, J. C., and Graves, J., Jr., "Laser-Induced Fluorescence Visualization of Transverse Gaseous Injection in a Nonreacting Supersonic Combustor," *Journal of Propulsion and Power*, Vol. 4, No. 6, 1988, pp. 591-597.
- ¹⁰Eggers, P. L., and Jackson, D. A., "Laser-Doppler Velocity Measurements in an Under-Expanded Free Jet," *Journal of Physics D: Applied Physics*, Vol. 7, 1974, pp. 1894-1906.
- ¹¹Hill, R. A., Peterson, C. W., Mulac, A. J., and Smith, D. R., "Enhanced Raman-Scattering Measurements in Low Density Supersonic Flows," *Journal of Quantitative Spectroscopy & Radiative Transfer*, Vol. 16, 1976, pp. 953-962.
- ¹²Yip, B., Lyons, K., Long, M., Mungal, M. G., Barlow, R., and Dibble, R., "Visualization of a Supersonic Underexpanded Jet by Planar Rayleigh Scattering," *Physics of Fluids A*, Vol. 1, No. 9, 1989, p. 1449.
- ¹³Hiller, B., and Hanson, R. K., "Simultaneous Planar Measurements of Velocity and Pressure Fields in Gas Flows Using Laser-Induced Fluorescence," *Applied Optics*, Vol. 27, No. 1, 1988, pp. 33-48.
- ¹⁴Miles, R. B., Connors, J., Markovitz, E., Howard, P., and Roth, G., "Instantaneous Supersonic Velocity Profiles in an Underexpanded Sonic Jet by Oxygen Flow Tagging," *Physics of Fluids A*, Vol. 1, No. 2, 1989, pp. 389-393.
- ¹⁵Escoda, M. C., and Long, M. B., "Rayleigh Scattering Measure-

ments of the Gas Concentration Field in Turbulent Jets," *AIAA Journal*, Vol. 21, No. 1, 1983, pp. 81-84.

¹⁶Bogdanoff, D. W., "Compressibility Effects in Turbulent Shear Layers," *AIAA Journal*, Vol. 21, No. 6, 1983, pp. 926-927.

¹⁷Tam, C. K. W., and Hu, F. Q., "On the Three Families of Instability Waves of High-Speed Jets," *Journal of Fluid Mechanics*, Vol. 201, 1989, pp. 447-483.

¹⁸McGregor, I., "The Vapor Screen Method of Flow Visualization," *Journal of Fluid Mechanics*, Vol. 11, No. 4, 1961, pp. 481-511.

¹⁹Samimy, M., and Lele, S. K., "Motion of Particles with Inertia in a Compressible Free Shear Layer," *Physics of Fluids* (to be published).

²⁰Dibble, R. W., Barlow, R. S., Mungal, M. G., Lyons, K., Yip, B., and Long, M. B., "Use of Rayleigh Scattering from Condensed

Water Vapor as a Means of Imaging an Underexpanded Supersonic Jet," STAR Meeting, Vanderbilt Univ., Nashville, TN, 1989.

²¹Sandham, N. D., "A Numerical Investigation of the Compressible Mixing Layer" Ph.D. Dissertation, Mechanical Engineering Dept., Stanford Univ., Stanford, CA, 1989.

²²Sandham, N. D., and Reynolds, W. C., "Growth of Oblique Waves in the Mixing Layer at High Mach Number," *Turbulent Shear Flows 7*, Stanford Univ., Stanford, CA, Aug. 21-23, 1989.

²³Ragab, S. A., and Wu, J. L., "Linear Instabilities in Two-Dimensional Compressible Mixing Layers," *Physics of Fluids A*, Vol. 1, No. 6, 1989, pp. 957-966.

²⁴Clemens, N. T., Mungal, M. G., Berger, T., and Vandsberger, U., "Visualizations of the Structures of the Turbulent Mixing Layer Under Compressible Conditions," AIAA Paper 90-0500, Jan. 1990.

Recommended Reading from the AIAA

Progress in Astronautics and Aeronautics Series . . .



Spacecraft Dielectric Material Properties and Spacecraft Charging

Arthur R. Frederickson, David B. Cotts, James A. Wall and Frank L. Bouquet, editors

This book treats a confluence of the disciplines of spacecraft charging, polymer chemistry, and radiation effects to help satellite designers choose dielectrics, especially polymers, that avoid charging problems. It proposes promising conductive polymer candidates, and indicates by example and by reference to the literature how the conductivity and radiation hardness of dielectrics in general can be tested. The field of semi-insulating polymers is beginning to blossom and provides most of the current information. The book surveys a great deal of literature on existing and potential polymers proposed for noncharging spacecraft applications. Some of the difficulties of accelerated testing are discussed, and suggestions for their resolution are made. The discussion includes extensive reference to the literature on conductivity measurements.

TO ORDER: Write, Phone or FAX:

American Institute of Aeronautics and Astronautics
c/o TASC0
9 Jay Gould Ct., P.O. Box 753, Waldorf, MD 20604
Phone (301) 645-5643, Dept. 415 • FAX (301) 843-0159

Sales Tax: CA residents, 7%; DC, 6%. For shipping and handling add \$4.75 for 1-4 books (call for rates for higher quantities). Orders under \$50.00 must be prepaid. Foreign orders must be prepaid. Please allow 4 weeks for delivery. Prices are subject to change without notice. Returns will be accepted within 15 days.

1986 96 pp., illus. Hardback
ISBN 0-930403-17-7

AIAA Members \$29.95

Nonmembers \$37.95

Order Number V-107